Quasi-One-Dimensional Magnetism Driven by Unusual Orbital Ordering in $CuSb_2O_6$

Deepa Kasinathan,[1] Klaus Koepernik,[1,2] and Helge Rosner[1]
[1]*Max-Planck-Institut für Chemische Physik fester Stoffe Dresden, Germany*
[2]*IFW Dresden, P.O. Box 270116, D-01171 Dresden, Germany*
(Received 11 April 2008; published 9 June 2008)

Essentially all undoped cuprates exhibit a quasiplanar, fourfold Cu-O coordination responsible for the magnetically active antibonding $3d_{x^2-y^2}$ like state. Here, we present an electronic structure study for $CuSb_2O_6$ that reveals, in contrast, a half-filled $3d_{3z^2-r^2}$ orbital. This hitherto unobserved ground state originates from a competition of in- and out-of-plaquette orbitals where the strong Coulomb repulsion drives the surprising and unique orbital ordering. This, in turn, gives rise to an unexpected quasi-one-dimensional magnetic behavior. Our results provide a consistent explanation of recent thermodynamical and neutron diffraction measurements.

DOI: 10.1103/PhysRevLett.100.237202 PACS numbers: 75.10.Lp, 71.15.Nc, 75.50.Dd

Low-dimensional systems have always been of fundamental interest to both experimentalists and theorists for their peculiar magnetic properties. In recent years, especially boosted by the discovery of the high-T_c superconductivity in cuprates, low-dimensional magnets related to this family of compounds have been widely studied. Low-dimensional cuprates exhibit a large variety of exotic physical properties. This variety is a result of the complex interplay of different interactions: mainly covalency, ligand-fields, and strong correlation effects.

A nearly universal component of cuprate systems is a strongly elongated CuO_6-octahedron [1] wherein the exotic behavior finds its origin in the deceivingly simple planar, half-filled Cu-O_4 orbital lying in its basal plane. Here, Cu $3d$ and O $2p$ states form a well-separated, half-filled $pd-\sigma$ molecularlike orbital of x^2-y^2 symmetry that is magnetically active. In general, the low-lying magnetic excitations, especially the magnetic ground state can be well described within this subspace of the whole Hilbert space. This way, the low-dimensional magnetic properties of a compound depend crucially on the arrangements of these Cu-O_4 units forming different networks, for instance (i) quasi 1D chains from isolated (i.e., $Sr_2Cu(PO_4)_2$ [2,3]) edge-sharing (i.e., Li_2CuO_2 [4,5]) or corner-sharing (i.e., Sr_2CuO_3 [6,7]) CuO_4 plaquettes, (ii) quasi 2D square lattices in La_2CuO_4 [8], etc.

In contrast to the vast majority of cuprates with a quasiplanar Cu(II) fourfold coordination, copper diantimonate $CuSb_2O_6$—first synthesized in early 1940s [9]—exhibits a nearly octahedral local environment of the Cu^{2+} ions. The compound is green in color [9,10], indicating insulating behavior with a gap size typical for cuprates. Although the compound undergoes a second order phase transition below 380 K from a tetragonal to a monoclinically distorted structure [11], this quasioctahedral local environment is basically unchanged. The magnetic cation sublattice is that of the K_2NiF_4 structure type, which includes many classic examples of square lattices exhibiting 2D antiferromagnetism (AFM), for instance the above mentioned La_2CuO_4. Surprisingly, susceptibility measurements done on both powder and single crystal samples of $CuSb_2O_6$ fit extremly well over a large temperature range to a nearest-neighbor--only $S=\frac{1}{2}$ Heisenberg 1D model with an exchange constant ranging from -86 K to -98 K [10,12–17]. Furthermore, all low temperature susceptibility measurements show a sharp drop at 8.5 K [10,12–16], due to the onset of long range AFM ordering [14–16]. Thus, the contrast of the 2D lattice and the 1D magnetic behavior in $CuSb_2O_6$ has been puzzling up to now.

In this Letter we present the combined results of the total energy and tight-binding model (TBM) calculations, which indicate an hitherto unobserved ground state originating from a competition between the in- and out-of-plaquette orbitals. Strong Coulomb correlation drives a surprising and unique orbital order in $CuSb_2O_6$, thereby leading to the strongly one-dimensional magnetic behavior with exchange integrals in good agreement with those deduced from experiments. Our results are consistent with recent neutron diffraction measurements [16].

The tetragonal structure [11] ($a=4.629$ Å, $c=9.288$ Å) of $CuSb_2O_6$ with 2 f.u. per unit cell is elucidated in Fig. 1. One interesting aspect of this system is the bond lengths, the out-of-plaquette Cu-O bond length is shorter by 0.04 Å compared to the in-plaquette Cu-O bond lengths. The CuO_6 octahedra are well separated from each other, with no edge sharing or corner sharing between adjacent CuO_6 octahedra. An angle $\beta \approx 91.2°$ is the main distinguishing factor of the monoclinic ($T<380$ K) phase of $CuSb_2O_6$. Nevertheless, the calculated density of states (DOS) and band structure for both these phases are nearly identical. Therefore, all band structure calculations shown here have been performed using the tetragonal trirutile structure instead of the monoclinic one for the sake of simplicity. Using the more regular tetragonal structure is quite advantageous in calculating and understanding the tight-binding hopping parameters and in the construction of larger supercells to model specific magnetic orderings.

We performed band structure calculations within the local (spin) density approximation (L(S)DA) using the

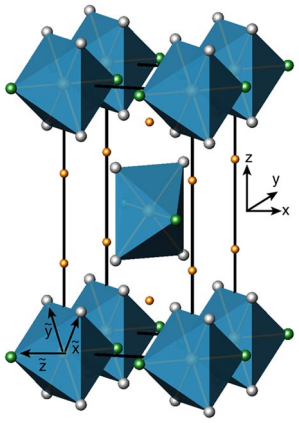

FIG. 1 (color online). The tetragonal trirutile structure of $CuSb_2O_6$. There are two Cu atoms per formula unit (two sublattices). The CuO_6 octahedra in these 2 sublattices are rotated by 90° with respect to each other. Both the global (x, y, z) and the local ($\tilde{x}$, $\tilde{y}$, $\tilde{z}$) coordinate systems used in our calculations are depicted. Within the local coordinate system, the in-plaquette oxygens are highlighted in gray while the out-of-plaquette oxygens are in green. The Sb atoms are highlighted in yellow. The in-plaquette Cu-O bondlength is 0.04 Å larger than the out-of-plaquette Cu-O bondlength.

full-potential local orbital minimum basis code FPLO (version 5.00–18) [18,19]. In the scalar relativistic calculations the exchange correlation potential of Perdew and Wang [20] was used. Additionally, the strong Coulomb repulsion in the Cu 3d orbitals was taken into account in a mean field approximation by LSDA + U calculations [21], using the around-mean-field double-counting scheme. Variations of U_d ($J = 1$ eV) within the relevant physical range ($U_d = 5$ to 9 eV) did not change the reported results significantly.

The calculated nonmagnetic LDA band structure, displayed in Fig. 2, shows four bands crossing the Fermi level E_F: i.e., two pairs of narrow and broad bands. Considering the 2 f.u. per cell, this is a very unusual result. In the standard cuprate scenario, only one well-separated half-filled antibonding band per Cu^{2+} is expected. Projecting the orbital character onto the band structure in a local coordinate system wherein the local $\tilde{z}$ axis is perpendicular to the Cu-O plaquette-plain (see Fig. 1) and points towards the apical oxygens, we find that the "narrow" bands originate from the in-plaquette Cu $d_{\tilde{x}^2-\tilde{y}^2}$ orbitals, while the "broad" bands come from the out-of-plaquette Cu $d_{3\tilde{z}^2-\tilde{r}^2}$ orbital. This is different from the conventional cuprate scenario where only one band per Cu atom crosses the Fermi level and is comprised predominantly of the in-plaquette Cu 3d orbital character. This unique feature stems from the fact that the CuO_6 octahedra are only slightly distorted in $CuSb_2O_6$, so that the cubic degeneracy for the e_g ligand-field states are only slightly lifted. The energy difference between the $d_{\tilde{x}^2-\tilde{y}^2}$ and $d_{3\tilde{z}^2-\tilde{r}^2}$ related band centers is about 0.3 eV only, to be compared with about 2 eV for "standard" cuprates.

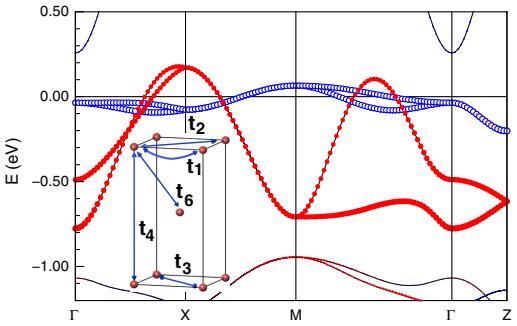

FIG. 2 (color online). LDA band structure of the tetragonal $CuSb_2O_6$ along high-symmetry directions. All four e_g bands are partially filled. The narrow band (open circle, blue) is entirely from the local Cu $d_{\tilde{x}^2-\tilde{y}^2}$ orbital, while the broad band (filled circle, red) comes from the Cu $d_{3\tilde{z}^2-\tilde{r}^2}$ orbital. The inset shows the leading hopping terms of the tight-binding model (see text).

Because of the strong competition between the in- and out-of-plaquette orbitals, the effects of strong correlations (LSDA + U) on the magnetic model are not immediately obvious. Let us first review the possible ways in which 1D order can be invoked in this system. Scenario 1: The interaction of the electrons is mediated via the CuO_4 plaquette, 1D chains will be formed along the $[1\bar{1}0]$ (and along [110] in the other sublattice). Scenario 2: The interaction of the electrons is mediated via the out-of-plaquette oxygen. This would in turn create 1D chains along the [110] (along $[1\bar{1}0]$ in the other sublattice) direction. These two competing scenarios in principle could lead to the same spin ordering pattern of 1D antiferromagnetic chains. Therefore strong correlations may drive the system to either one of these two scenarios.

First, to compare the microscopic magnetic interactions in $CuSb_2O_6$, we did a two-site one-band TBM fit, separately for the $d_{\tilde{x}^2-\tilde{y}^2}$ and $d_{3\tilde{z}^2-\tilde{r}^2}$ band complexes. The respective 2×2 tight-binding matrix is given by

$$\begin{pmatrix} \alpha + \beta & \delta \\ \delta & \alpha + \beta' \end{pmatrix},$$

with

$$\alpha = \epsilon_0 + 2t_1[C_{\tilde{x}} + C_{\tilde{y}}] + 2t_4 C_{\tilde{z}} + 4t_5[C_{\tilde{x}} + C_{\tilde{y}}]C_{\tilde{z}},$$

$$\beta = 2t_2[C_{\tilde{x}}C_{\tilde{y}} - S_{\tilde{x}}S_{\tilde{y}}] + 2t_3[C_{\tilde{x}}C_{\tilde{y}} + S_{\tilde{x}}S_{\tilde{y}}],$$

$$\beta' = 2t_3[C_{\tilde{x}}C_{\tilde{y}} - S_{\tilde{x}}S_{\tilde{y}}] + 2t_2[C_{\tilde{x}}C_{\tilde{y}} + S_{\tilde{x}}S_{\tilde{y}}],$$

$$\delta = 8t_6 C_{(1/2)\tilde{x}}C_{(1/2)\tilde{y}}C_{(1/2)\tilde{z}} + 8t_7 C_{(1/2)\tilde{z}}[C_{(3/2)\tilde{x}}C_{(1/2)\tilde{y}} - C_{(1/2)\tilde{x}}C_{(3/2)\tilde{y}}],$$

where $C_{\tilde{x}} = \cos(k_{\tilde{x}}a)$, $C_{(1/2)\tilde{x}} = \cos(k_{\tilde{x}}\frac{a}{2})$, $C_{(3/2)\tilde{x}} = \cos(k_{\tilde{x}}\frac{3a}{2})$, $S_{\tilde{x}} = \sin(k_{\tilde{x}}a)$ and the corresponding cyclic permutations. The values of the transfer integrals obtained from the fit are collected in Table I, with the hopping paths shown in the inset of Fig. 2. The hopping parameters obtained from the fit to the narrow $d_{\tilde{x}^2-\tilde{y}^2}$ band complex are all quite similar in magnitude, implying almost equal interaction strength along the three main hopping paths t_1,

t_3, and t_4 (see Table I. This is indicative of a 3D magnetic model and the energy scale of the transfer integrals are too small. This 3D model is incompatible with the experimental data [16]. The fit to the broad $d_{3\tilde{z}^2-\tilde{r}^2}$ band produces a transfer integral (t_2) which is very large compared to all others (see Table I). This suggests a strong 1D AFM interaction along the [110] direction, implying that the superexchange path Cu-O-O-Cu is along the [110] basal diagonal and is via the apical oxygens and not via the in-plaquette oxygens. This is in line with the band characters of the projection mentioned above. This leads to almost perfect 1D chains of antiferromagnetic Cu atoms along the [110] direction. Another interesting fact to notice is the difference in the next-nearest-neighbor interaction along [110] (t_2) and [$\bar{1}$10] (t_3). The Cu-O bondlength along [110] is shorter (2 Å) with a 180° bond angle as compared to the Cu-O bond length of 3.5 Å along [$\bar{1}$10] and a 160° Cu-O-Cu bond angle. This structural feature also helps in the one dimensionality along [110]. The individual exchange constants calculated using $J_{ij} = 4t_{ij}^2/U_{\text{eff}}$, with a $U_{\text{eff}} = 4.5$ eV [22] are also collected in Table I. The sublattice coupling, connecting the two Cu sites in the unit cell is rather small, but not negligible, and so are the interchain couplings. This is very much consistent with the 1D nature of the system. Though the plaquettes are quite isolated in $CuSb_2O_6$, they can interact in many different ways and this in turn determines the magnitude of the exchange constants. But the unique geometry in this system gives a very large 1D exchange ($J_2^{\text{TBM}} = 400$ K) as compared to other 2D cuprates. This value of J_2 is too large (by a factor of 4) due to possible ferromagnetic contributions like in other cuprate compounds. We perform LSDA + U calculations to get a deeper insight.

Within LSDA + U, depending on the choice of the input density matrix, we were able to correlate (fill the spin-up band and unfill the spin-down band) both band complexes in the vicinity of the Fermi level. Contrary to other typical cuprates, the ground state is obtained when correlating the "broad" Cu $d_{3\tilde{z}^2-\tilde{r}^2}$ orbital (i.e., $d^{\uparrow}_{\tilde{x}^2-\tilde{y}^2}$, $d^{\downarrow}_{\tilde{x}^2-\tilde{y}^2}$, $d^{\uparrow}_{3\tilde{z}^2-\tilde{r}^2}$: filled and $d^{\downarrow}_{3\tilde{z}^2-\tilde{r}^2}$: empty) with an energy gain of about 110 meV (~1280 K) [23] per Cu atom as compared to the "narrow" $d_{\tilde{x}^2-\tilde{y}^2}$ orbital (i.e., $d^{\uparrow}_{3\tilde{z}^2-\tilde{r}^2}$, $d^{\downarrow}_{3\tilde{z}^2-\tilde{r}^2}$, $d^{\uparrow}_{\tilde{x}^2-\tilde{y}^2}$: filled and $d^{\downarrow}_{x^2-y^2}$: empty). This result is in accordance with the second scenario described above and also with the 1D TBM result. Superexchange via the apical Cu-O orbitals is quite surprising and unique, though not categorically excluded. Since the apical Cu-O bondlength is slightly shorter than the in-plaquette one, the covalency of Cu with the apical oxygens are slightly larger than that with the planar oxygens. We can also notice from the LDA band structure (Fig. 2) that the $d_{\tilde{x}^2-\tilde{y}^2}$ band is quite narrow compared to $d_{3\tilde{z}^2-\tilde{r}^2}$ band. Keeping this in mind, we can interpret the unique orbitally ordered ground state to be the result of the relative gain in kinetic energy when correlating the broad Cu $d_{3\tilde{z}^2-\tilde{r}^2}$ orbital.

Our TBM for the Cu $d_{3\tilde{z}^2-\tilde{r}^2}$ orbitals results in very short-ranged interactions (Table I). Therefore an extension of the supercells beyond the second neighbors is not necessary. LSDA + U calculations of differently ordered spin configurations (FM and AFM) were performed to obtain an effective exchange constant, J_2^{nn} by mapping the energies obtained from the calculations to a Heisenberg model (neglecting the other J's since they are small according to the TBM), $H = \sum_{\langle i,j\rangle} J_{ij}\mathbf{S}_i \cdot \mathbf{S}_j$ which leads to $E_{\text{fm}} - E_{\text{afm}} = 2J_2^{nn}|S|^2$, $S = \frac{1}{2}$. This model leads to $J_2^{nn} \sim 140$ K, in good comparison to the value of about 100 K obtained in susceptibility experiments [16]. The slight overestimation of the leading exchange is rather typical for this type of calculation [3] and also somewhat dependent on the choice of U which is not exactly known. We obtain a charge transfer gap of 2.2 eV which is consistent with the green color of the sample.

The presence of quite regular octahedra in $CuSb_2O_6$ introduces an orbital degree of freedom among the e_g orbitals as compared to other standard cuprates. Electronic structure calculations give convincing evidence for the strong competition between the $d_{\tilde{x}^2-\tilde{y}^2}$ and $d_{3\tilde{z}^2-\tilde{r}^2}$ orbitals for the ground state in $CuSb_2O_6$. Correlations drive a unique $d_{3\tilde{z}^2-\tilde{r}^2}$ orbital ordering pattern in the ground state (Fig. 3). Our TBM and total energy calculations (mapped onto an effective Heisenberg Hamiltonian) are in favor of a 1D ($d_{3z^2-r^2}$) instead of 3D ($d_{x^2-y^2}$) scenario following a particular orbital ordering. Our ordering pattern is consistent with the magnetic unit cell proposed from the results of neutron diffraction experiments [10,16]. This in turn elucidates that the low-lying excitations for cuprates are not restricted *a priori* to the standard orbital picture.

The analysis above has only considered the isotropic superexchange interaction. Allowing for spin-orbit coupling introduces anisotropic terms in the superexchange interaction. Many model calculations have been performed for various cuprates to determine the magnetic anisotropy energy [24], which scales inversely with the difference

TABLE I. Hopping parameters and the corresponding exchange constants from a two-site one-band TBM. The hopping paths used are: $t_1[000] \rightarrow [100]$, $t_2[000] \rightarrow [110]$, $t_3[000] \rightarrow [\bar{1}10]$, $t_4[000] \rightarrow [001]$, $t_5[000] \rightarrow [101]$, $t_6[000] \rightarrow [\frac{1}{2}\,\frac{1}{2}\,\frac{1}{2}]$, $t_7[000] \rightarrow [\frac{3}{2}\,\frac{1}{2}\,\frac{1}{2}]$. The hopping paths are indicated in the inset of Fig. 2. The fit has been done for both the in-plaquette $d_{\tilde{x}^2-\tilde{y}^2}$ and the out-of-plaquette $d_{3\tilde{z}^2-\tilde{r}^2}$ bands separately. The parameters are vanishingly small when no value is provided.

(meV)	t_1	t_2	t_3	t_4	t_5	t_6	t_7
$d_{x^2-y^2}$	−20	⋯	17.5	20.8	3.80	⋯	−1.86
$d_{3z^2-r^2}$	9.52	−197	−13.1	−3.86	⋯	−17.9	⋯

(K)	J_1	J_2	J_3	J_4	J_5	J_6	J_7
$d_{x^2-y^2}$	4.23	⋯	3.15	4.46	0.15	⋯	0.04
$d_{3z^2-r^2}$	0.93	400	1.76	0.15	⋯	3.32	⋯

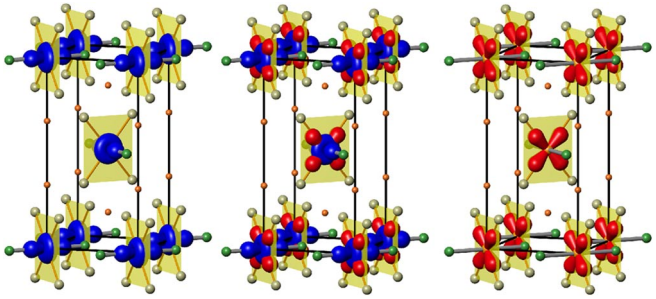

FIG. 3 (color online). Middle panel: The competition of in-plaquette and out-of-plaquette orbitals in LDA for $CuSb_2O_6$. Both orbitals are partially occupied and comprise the Fermi surface. Right panel: Standard picture of high T_c cuprates with the inclusion of strong Coulomb correlations U. The plaquette orbitals remain half-filled and thereby would lead to 3D magnetic order. Left panel: Unique orbital ordering in $CuSb_2O_6$ leading to a strong 1D magnetic order.

between the $d_{x^2-y^2}$ and $d_{3z^2-r^2}$ energy levels. Contrary to other cuprates, this energy difference in $CuSb_2O_6$ is extremely small due to the presence of a rather regular octahedron. Therefore, we can qualitatively infer that $CuSb_2O_6$ exhibits a large magnetic anisotropy. This anisotropy reduces the phase space of the isotropic Heisenberg model and should lead to a significant increase of the magnetic ordering temperature. Indeed, if we estimate the Néel temperature (T_N) assuming an isotropic $S = \frac{1}{2}$ quasi-one-dimensional chain within the bosonization method [25,26],

$$T_N = 0.33kJ'z_\perp\sqrt{\ln\frac{5.8J}{T_N} + \frac{1}{2}\ln\ln\frac{5.8J}{T_N}}$$

we find $T_N^{\text{theo}} \approx 1.5$ K which strongly underestimates the observed $T_N^{\text{expt}} \approx 8.5$ K. Because of the mean fieldlike treatment of the interchain coupling, T_N^{theo} is expected to be an upper estimate [7]. The strong underestimation of the ordering temperature using the isotropic model implies the presence of considerable anisotropy in the system, which is naturally explained by our orbital scenario.

In conclusion, electronic structure and TBM calculations in $CuSb_2O_6$ reveal 1D behavior from orbital ordering due to a competition between the Cu $d_{\tilde{x}^2-\tilde{y}^2}$ and $d_{3\tilde{z}^2-\tilde{r}^2}$ orbitals; strong Coulomb repulsion selects the latter (Fig. 3). The main reason for such a ground state is the underlying local environment. Our results are in agreement with the susceptibility and recent neutron diffraction measurements for the spin structure [16]. Performing polarization dependent x-ray absorption spectroscopy (XAS) should elucidate the choice of orbital ordering in $CuSb_2O_6$. A strong anisotropy in the absorption edge will be observed when using the incoming radiation $E \parallel \mathbf{a}$-$\mathbf{b}$ plane as compared to $E \parallel \mathbf{c}$. We are currently analyzing the results from this experiment. Effects of pressure on this system are quite interesting, as they can flip the balance between the two competing orbitals thereby restoring the standard plaquette picture as in other cuprates.

We acknowledge critical remarks from A. Ormeci, W. Ku, M. D. Johannes. Funding from the Emmy-Noether program is acknowledged.

[1] H. Müller-Bauschbaum, Angew. Chem. **89**, 704 (1977).
[2] A. A. Belik *et al.*, J. Solid State Chem. **178**, 3461 (2005).
[3] M. D. Johannes, J. Richter, S.-L. Drechsler, and H. Rosner, Phys. Rev. B **74**, 174435 (2006).
[4] R. Weht and W. E. Pickett, Phys. Rev. Lett. **81**, 2502 (1998).
[5] H. Rosner, R. Hayn, and S.-L. Drechsler, Physica (Amsterdam) **261B**, 1001 (1999).
[6] T. Ami *et al.*, Phys. Rev. B **51**, 5994 (1995).
[7] H. Rosner *et al.*, Phys. Rev. B **56**, 3402 (1997).
[8] G. Shirane *et al.*, Phys. Rev. Lett. **59**, 1613 (1987).
[9] A. Bystrom, B. Hok, and B. Mason, Ark. Kemi Mineral. Geol. B **15**, 1 (1941).
[10] A. Nakua *et al.*, J. Solid State Chem. **91**, 105 (1991); A. M. Nakua and J. E. Greedan, J. Solid State Chem. **118**, 199 (1995).
[11] E.-O. Giere *et al.*, J. Solid State Chem. **131**, 263 (1997).
[12] Masaaki Yamaguchi *et al.*, J. Phys. Soc. Jpn. **65**, 2998 (1996).
[13] Masaki Kato *et al.*, Physica (Amsterdam) **281–282B**, 663 (2000); J. Phys. Chem. Solids **63**, 1129 (2002).
[14] M. Heinrich *et al.*, Phys. Rev. B **67**, 224418 (2003).
[15] A. V. Prokofiev *et al.*, J. Cryst. Growth **247**, 457 (2003).
[16] B. J. Gibson *et al.*, J. Magn. Magn. Mater. **272–276**, 927 (2004).
[17] All the experimental exchange constants have been normalized to sum over bonds to aid easy comparison to our results.
[18] K. Koepernik and H. Eschrig, Phys. Rev. B **59**, 1743 (1999).
[19] The extension of valence orbitals (Cu $3d4s4p$, Sb $5s5p5d$, and O $2s2p3d$) were optimized with respect to total energy using an additional confining potential $(r/r_0)^4$.
[20] J. P. Perdew and Y. Wang, Phys. Rev. B **45**, 13244 (1992).
[21] M. T. Czyżyk and G. A. Sawatzky, Phys. Rev. B **49**, 14211 (1994).
[22] For the isolated CuO_6 geometry we use a representative $U_{\text{eff}} = 4.5$ eV according to reference [3].
[23] Comparing this energy gain (1276 K) for correlating the Cu $d_{3\tilde{z}^2-\tilde{r}^2}$ orbital with that of $J_2^{\text{TBM}} = 400$ K, allows for the separation of the spin and orbital degrees of freedom due to varied energy scales.
[24] V. Yu. Yushankhai and R. Hayn, Europhys. Lett. **47**, 116 (1999).
[25] V. Yu. Irkhin and A. A. Katanin, Phys. Rev. B **61**, 6757 (2000).
[26] $z_\perp = 4$ is the number of neighbors in transverse to chain directions and k for a tetragonal lattice (dimension $d = 1 + 2$) is set to 0.7 [25]. The variable J denotes the leading coupling along the direction of the chain, set equal to $J_{\text{expt}} = 100$ K, and J' denotes nonfrustrating interchain coupling, set equal to $\sqrt{J_3 J_4} = 0.5$ K, using the results from our TBM following the procedure of Ref. [7].